Frontiers in Bioscience Landmark

Front. Biosci. (Landmark Ed) **2022**; 27(11): 308
https://doi.org/10.31083/j.fbl2711308

Original Research

Antioxidant Activity of Cyanidin-3-O-Glucoside and Verbascoside in an *in Vitro* Model of Diabetic Retinopathy

Carmelina Daniela Anfuso[1,†], Giovanni Giurdanella[1,2,†], Anna Longo[1], Alessia Cosentino[1], Aleksandra Agafonova[1], Dario Rusciano[3,*], Gabriella Lupo[1]

[1]Department of Biomedical and Biotechnological Sciences, School of Medicine, Section of Medical Biochemistry, University of Catania, 95123 Catania, Sicilia, Italy
[2]Faculty of Medicine and Surgery, University of Enna "Kore", 94100 Enna, Sicilia, Italy
[3]Fidia-Ofta Research Center c/o Department of Biomedical and Biotechnological Sciences, Catania University, 95123 Catania, Sicilia, Italy
*Correspondence: drusciano55@gmail.com (Dario Rusciano)
[†]These authors contributed equally.
Academic Editor: Graham Pawelec
Submitted: 23 July 2022 Revised: 8 November 2022 Accepted: 9 November 2022 Published: 17 November 2022

Abstract

Background: Reactive oxygen species (ROS) accumulation plays a pivotal role in the onset of cell damage induced by hyperglycemia and represents one of the major factors in the pathogenesis of diabetic retinopathy. In this study, we tested the antioxidants cyanidin-3-O-glucoside (C3G) and verbascoside (Verb) in the protection of retinal endothelium against glucose toxicity "*in vitro*". **Methods**: Increasing amounts (5–50 μM) of C3G, Verb or the combination of both compounds were tested in Human Retinal Endothelial Cells (HREC) grown with normal glucose (5 mM, NG) or high glucose (25 mM, HG). **Results**: Reduced cell viability and enhanced ROS levels (evaluated by MTT and H2DCFDA assays, respectively) in HG-stimulated HREC were restored by C3G and Verb in a dose-dependent manner, achieving the maximum protection in the presence of both compounds. Moreover, co-treatment with C3G and Verb worked better than each single molecule alone in the prevention of the disruption of blood-retinal-barrier-like properties by HG in a confluent HREC monolayer, as assessed by trans endothelial electrical resistance (TEER) and Na-Fluorescein permeability assays. Accordingly, C3G and Verb together also better counteracted the HG-induced down-regulation of the tight junction membrane proteins Zonula Occludens-1 and VE-Cadherin evaluated by immunocytochemical and Western blot analyses. **Conclusions**: In conclusion, our data indicate that C3G and Verb could efficiently protect the retinal endothelium against high glucose damage.

Keywords: cyanidin-3-O-glucoside; verbascoside; high glucose; retinal endothelial cells; VE-Cadherin; Zonula Occludens-1; Na-Fluorescein permeability assay; reactive oxygen species

1. Introduction

Diabetic retinopathy (DR) is a common retinal microvascular complication occurring in diabetic patients, often leading to vision loss and blindness [1,2]. Clinical manifestations of DR are classified in two main stages: the earliest stage being non-proliferative diabetic retinopathy (NPDR) and the more advanced stage being proliferative diabetic retinopathy (PDR). A prolonged poor glycemic control triggers NPDR characterized by increased vascular permeability, capillary occlusion, microaneurysms, hemorrhages and hard exudates [3]. The progressive breakdown of the inner blood-retinal barrier (iBRB) can contribute to the formation of diabetic macular edema (DME), which is the most common cause of vision impairment in DR, through subretinal and intraretinal accumulation of fluid leading to the swelling of the macula [4]. The production of new abnormal vessels due to neovascularization processes represents the main clinical hallmark of PDR that worsens DR symptoms by bleeding into the vitreous and inducing retinal detachment and severe vision impairment [5]. Chronic exposure to hyperglycemia drives the early microvascular damage through an excessive production of advanced glycation end products (AGEs) and the aberrant activation of polyol, hexosamine and protein kinase C (PKC) pathways [6,7]. These activated pathways lead to increased levels of oxidative stress in retinal cells resulting from an altered balance between reactive oxygen species (ROS) production and the cellular antioxidant defense system. This includes enzymes, such as superoxide dismutase (SOD), heme oxygenase, and catalase [8,9], as well as nonenzymatic antioxidant agents such as uric acid, bilirubin and glutathione including vitamins (E and C) and polyphenols, all aimed at protecting cells through a direct scavenging activity of free radicals [10]. However, hyperglycemia-induced metabolic changes trigger the generation of an overwhelming amount of ROS from several pathways including the mitochondrial electron transportation chain, and the increased activity of NADH oxidase, cytochrome P450 and xanthine oxidase [11–13]. Moreover, the excessive consumption of NADPH produced by the activation of the polyol pathway decreases glutathione (GSH) synthesis, contributing to the alteration of the homeostatic redox system and the increase

of intracellular ROS [11,14,15]. Oxidative damage induced by ROS accumulation underlies multiple pathological processes in DR such as lipid peroxidation and mitochondrial dysfunction, finally leading to apoptosis and progressive endothelial abnormalities [16–19]. ROS were shown to promote inflammatory processes through the production of cytokines such as tumor necrosis factor-alpha (TNF-α), interleukin-1-beta (IL-1β), and interleukin-6 (IL-6), mediated by nuclear factor (NF)-kappa B (NF-κB) transcription factor activation [20–22]. BRB breakdown during the pathogenesis of DR is tightly correlated to the dysregulation of cell junction-associated proteins such as VE-cadherin and Zonula Occludens-1 (ZO-1), which were shown to be downregulated as a consequence of NF-κB activation or VEGF up-regulation [23,24]. The critical involvement of VE-cadherin in the disruption of the BRB has been clearly demonstrated in diabetic rats, and shown to be—at least partially—the consequence of enhanced proteolytic digestion by activated MMPs [25]. Overall, the establishment of early vascular inflammatory status induced by oxidative damage underlies the onset of DR and promotes its advanced stages. Based on this evidence, an increasing number of investigations regarding the benefit of enhanced ROS suppression by using food supplements have been published during the last few decades [26,27].

Anthocyanins were proposed as promising nutraceutical molecules for the prevention of DR via their antioxidant and anti-inflammatory properties [28,29]. Among anthocyanins, cyanidin-3-O-glucoside (C3G) represents a powerful natural antioxidant with beneficial effects in cases of increased oxidative stress, and at pharmacological concentrations it has been shown to be able to decrease tissue damage occurring in myocardial ischemia and reperfusion [30]. C3G also prevented the hyperglycemia-induced hepatic oxidative damage by activating GSH synthesis against ROS production [31]. Moreover, C3G showed a protective scavenging activity against endothelial dysfunction and vascular failure induced by peroxynitrite [32]. Besides the antioxidant activity, C3G could enhance vascular eNOS activity, thus contributing to improve vascular endothelial function [33].

Verbascoside (Verb, a.k.a. acteoside), a molecule belonging to the phenylpropanoid family, was discovered in extracts from *Verbascum sinuatum* L. in 1950, and found to be largely diffused in other dietary plants and fruits, such as pigmented oranges that are very common in the Mediterranean diet [34,35]. The antioxidant capacity of Verb is related to its free radical scavenging ability, leading to antihypertensive, anti-cancer and neuroprotective effects [36–40]. Verb reduced platelet aggregation in patients with cardiovascular risk factors and enhanced the anti-aggregating activity of aspirin after adenosine diphosphate (ADP) stimulation [41,42], thus improving blood perfusion.

Recently, it has been hypothesized that an enhanced antioxidant activity can be achieved through a cooperative interaction among different antioxidant constituents as they may exert multi-target effects activating or modulating different pathways involved in redox homeostasis [43,44]. For instance, the association of C3G and Verb has been shown to protect the retina from different types of insults and oxidative stress. In a rat model of light-induced photooxidative retinal damage, oral pretreatment with a mixture containing C3G, Verb, lutein and zinc protected photoreceptor cells from death by preventing oxidative stress, inflammation, gliotic and apoptotic responses. The better efficacy of the mixture on the dysfunctional electroretinogram was also demonstrated by the improved rod and cone photoreceptor responses [45]. More pertinent to the goal of this study is the efficacy shown by the oral administration of the association of C3G, verbascoside and zinc on the diabetic retinopathy induced in rats by streptozotocin treatment [46]. This *in vivo* preclinical study reported a dose-dependent inhibition of oxidative stress-related and inflammation-related mechanisms in the retina of diabetic rats, with a significant reduction of DR-associated vasculopathy and its related retinal damage. Electroretinography under photopic and scotopic conditions also demonstrated the preventive efficacy of the compound on dysfunctional a-waves and b-waves.

Therefore, based on this preliminary evidence, we set out to evaluate in this study the antioxidant and protective effects of C3G and Verb, either alone or in association, on the dysfunction of the endothelial barrier triggered by high glucose in an *in vitro* model of DR obtained by treating human retinal endothelial cell (HREC) monolayers with high concentrations of glucose (25 mM).

2. Materials and Methods

2.1 Reagents

Cyanidin-3-glucoside (Black Rice Extract 20, Bionap, Italy) and verbascoside (Verbalief, Bionap, Italy) were kindly donated by 'La Sorgente del Benessere' (Fiuggi, Italy). Antibodies against tight junction proteins were: rabbit polyclonal ZO-1 antibody (Thermo Fisher Scientific, Waltham, MA, USA); rabbit monoclonal VE-cadherin antibody (Cell Signaling Technology, Danvers, MA, USA). Reagents for cell cultures were from Invitrogen Life Technologies (Carlsbad, CA, USA).

2.2 Cell Culture and Treatments

Primary human retinal endothelial cells (HREC) were purchased from Innoprot (Derio-Bizkaia, Spain) and cultured with endothelial cell medium (ECM) supplemented with 5% fetal bovine serum (FBS), 1% endothelial cell growth supplement (ECGS), 100 U/mL penicillin and 100 μg/mL streptomycin, all purchased from Innoprot. HREC were used between 3 and 12 passages. Throughout this interval, HREC expressed high levels of immunostaining with von Willebrand factor (Fig. 1), as expected [47]. Before cell seeding, flasks or dishes were pre-coated with bovine plasma fibronectin (Innoprot) at a concentration of

1 mg/mL for 1 h in a humidified atmosphere of 5% CO_2 at 37 °C and subsequently rinsed twice with sterile distilled water. Before treatments, HREC were adapted to ECM medium with 2.5 % FBS for 24 h. Then, cells were incubated under control conditions (NG, 5 mM) or with 25 mM glucose (HG) in 2.5 % FBS ECM medium up to 72 h with different concentrations of C3G (5, 10 and 50 μM), Verb (5, 10 and 50 μM) or a combination of C3G and Verb (5, 10 and 50 μM each) for 48 h. Cell treatments were started on cell monolayers at about 70% confluence. C3G and/or Verb were added at the same time when the new medium with NG or HG was replaced in culture wells.

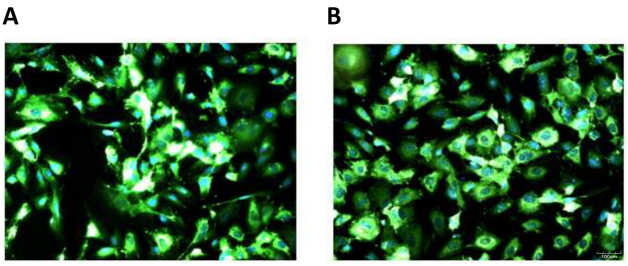

Fig. 1. Von Willebrand staining. HREC at passage 3 (A) and 9 (B) were immunostained for the endothelial molecular marker von Willebrand factor, showing similar morphologies and staining intensity, indicating a reliable stability of the endothelial phenotype.

2.3 Cell Viability

Cell viability was determined by the metabolic MTT colorimetric assay (Cell Counting Kit 8 (CCK8) reagent) (Sigma-Aldrich, St. Louis, MO, USA), based on the reduction of a yellow tetrazolium salt (3-(4,5-dimethylthiazol-2-yl)-2,5-diphenyltetrazolium bromide or MTT) to purple formazan crystals by metabolically active cells. HREC were seeded at 1.5 $\times$ 10^4 cells per well into 96-well plates. After overnight growth, cells were treated under different conditions and with the different agents, as described above (section 2.2). At the end of treatment, 10 μL of the CCK8 solution was added to 90 μL of culture medium, and the cells incubated for 4 h at 37 °C. Optical absorbance of the colored medium was measured at 450 nm using a microplate reader (Varioskan, Thermo Fisher Scientific, Waltham, MA, USA).

2.4 ROS Measurements

Reactive oxygen species (ROS) were measured by means of the DCFDA Cellular ROS Detection Assay Kit (ab113851, Abcam Cambridge, UK), according to the manufacturer's protocol. After treatments with HG or NG, HREC were incubated with 25 μM 2′,7′-dichlorodihydrofluorescein diacetate (DCFDA) in a buffer solution at 37 °C for 30 min. Then, DCFDA was replaced with 100 μL of ECM and the fluorescence intensity (λex = 492 nm, λem = 517 nm) directly correlating with ROS amount was measured with the VarioskanTM (Thermo Fisher Scientific, Waltham, MA, USA).

2.5 Transendothelial Electrical Resistance Measurement

HREC were plated in transwells (Costar, 3412) with $\times$ 0.4 μm pores at the density of 7 $\times$ 10^4 cells/cm^2. Transendothelial electrical resistance (TEER) was measured with the Millicell-ERS system (MERS 000 01; Millipore, AG, Volketswil, Switzerland) as described [48]. Blank values on empty transwells were recorded. Experimental values were expressed as $\omega \times cm^2$ and were calculated by the formula: [average resistance of experimental wells – average resistance of blank wells] $\times$ 0.33 (the area of the transwell membrane). In order to achieve optimal HREC confluent monolayers, TEER values were monitored for 3–4 days before the challenge with different treatments. TEER measurement was carried out in transwells containing a confluent HREC monolayer and treated with NG or with HG in 2.5% FBS ECM medium with or without C3G (50 μM), Verb (50 μM) or a combination of C3G and Verb (50 μM each) during 72 h of treatment.

2.6 Transendothelial Permeability of Sodium Fluorescein

The diffusion of sodium fluorescein (Na-F, Santa Cruz Biotechnology, cat. number sc206026) across HREC monolayers was determined as previously described [49]. HREC confluent monolayers were grown in transwells until reaching barrier properties and then were treated with NG or with HG in 2.5% FBS ECM medium with or without C3G (50 μM), Verb (50 μM) or a combination of C3G and Verb (50 μM each) for 48 h. Subsequently, the transwells were transferred into 12-well plates containing 1.0 mL of the Ringer–Hepes buffer in the basolateral compartments. The culture media contained within the transwells (apical compartments) was replaced with 0.5 mL of Ringer–Hepes buffer supplemented with 100 mg/mL of sodium fluorescein (Na-F, m.w. 376 Da). Na-F flux from apical to basolateral compartments was evaluated by measuring the fluorescence of the marker molecule in samples taken from the upper and lower compartments after 5, 15, and 30 min. Flux across cell-free inserts was also measured. Na-F concentrations were determined with a fluorescence multiwell plate reader (excitation: 485 nm, emission: 535 nm). The transendothelial permeability coefficient (P_e expressed as 10^{-6} cm/s) was calculated as previously described [50]:

$$P_e = C_B/T \times 1/F \times V_B/C_U$$

Where C_B is the fluorescein concentration measured in the bottom well in mg/mL; T is the time of measurement expressed in seconds; F is the filter area on which the cells are grown (1 cm^2 in our case); V_B is the volume of the bottom well (1.0 mL in our case); C_U is fluorescein concentration in the upper well (100 mg/mL).

The correlation coefficient between TEER values and Pe in the different experimental conditions was calculated with GraphPad Prism 7 for Windows using the function linear fit dose-response interpolation.

2.7 Immunocytochemical Analysis

Immunostaining of HREC with rabbit polyclonal antibodies against Von Willebrand Factor (Abcam, Cambridge, UK; catalog num. ab6994) was done on cells at passage 3 or 9. Cells were seeded on poly-L-lysine precoated glass coverslips in a 24-well plate, at 2×10^4 cells/well and incubated for 2 days at 37 °C in a humidified atmosphere of 5% CO_2. Next, cells were incubated overnight at 4 °C with the primary antibody (1:120) in a PBS/triton 0.1% solution. The following day, cells were washed with PBS and incubated for 1 h at room temperature with the secondary antibody, goat anti-rabbit FITC-conjugated. Immunocytochemical analysis of junction-related proteins ZO-1 and VE-Cadherin was done as following. Sterile glass chamber slides were placed in wells of a 24-multiwell plate, and coated with bovine plasma fibronectin at a concentration of 1 mg/mL (Innoprot) for 1 h at 37 °C. After washing with sterile water, they were seeded with HREC in ECM with 2.5% FCS at a cell density of 5×10^4 cells/well, and incubated for 24 h in a humidified atmosphere of 5% CO_2 at 37 °C. Then, cells were incubated for a further 48 h under control conditions (NG, 5 mM) or shifted to 25 mM glucose (HG), with or without 50 μM each of C3G and Verb together. After the incubation period, the cells were fixed at room temperature with ice-cold acetone for 15 min followed by ice-cold methanol for 20 min and then washed several times in PBS. Fixed cells were then incubated with rabbit polyclonal primary antibodies for ZO-1 or VE-Cadherin diluted (1:150) in PBS/Triton 0.1%, overnight at 4 °C. After washing three times in PBS, cells were incubated for 1 h with the anti-rabbit Alexa 488-conjugated secondary antibody (1:300 dilution, Life Technologies, A32731) at room temperature in the dark. After three further washings with PBS, slides were finally mounted using the mounting medium (Life Technologies) containing DAPI for nuclei staining and observed with a fluorescence microscope Zeiss Observer Z1 equipped with the Apotome.2 acquisition system connected to a digital camera (Carl Zeiss, Oberkochen, Germany).

2.8 Western Blot Analysis

After treatments under different conditions with NG or HG, cellular monolayers were washed twice with PBS and harvested mechanically, using a cell scraper. Cells were centrifuged at 1000 rpm for 5 min at 25 °C, and pellets were lysed in RIPA buffer (Calbiochem-Merck, 20188, Darmstadt, Germany) supplemented with protease and phosphatase inhibitor cocktails (Protease Inhibitor Cocktail Set III EDTA-Free, Calbiochem-Merck, 539134; Phosphatase Inhibitor Cocktail 2, Sigma Aldrich, P5726, USA; Phosphatase Inhibitor Cocktail 3, Sigma Aldrich, P0044, USA) by incubation for 30 min on ice. Extracts were clarified by centrifugation at 13,000 rpm for 20 min at 4 °C, and proteins in the supernatant quantitated by the BCA protein assay (BCA kit assay, Santa Cruz biotechnology, 10410, Dallas, TX, USA). For Western blot analysis, 40 μg of proteins were loaded onto a 4–20% polyacrylamide gel (Mini-PROTEAN® TGXTM Precast Protein Gels, 4561096, Bio-Rad Laboratories, Segrate, Milano, Italy) followed by electrotransfer to nitrocellulose membranes (Trans-Blot Turbo Mini 0.2 μm nitrocellulose, 1704158, Bio-Rad Laboratories, Italy). Membranes were blocked for 30 min with Odyssey Blocking Buffer (LI-COR Biosciences, Lincoln, NE, USA), and then incubated overnight at 4 °C with primary antibodies against ZO1 or VE-Cadherin diluted 1:1000. After a thorough washing of the membranes, incubation with IgG-HRP-conjugated anti-rabbit secondary antibodies (Amersham, GE Healthcare, Illinois, USA, NA934V) diluted 1:2000 was done for 1 h at room temperature. As loading control, we used the rabbit monoclonal GAPDH antibody (1:1000, Cell Signaling Technology, 2118, Danvers, MA, USA). Immunoblots were detected by using Odyssey Imaging System (LI-COR Biosciences, Lincoln, NE, USA). The intensity of protein bands was quantitated by ImageJ Software (NIH, Bethesda, MD, USA).

2.9 Statistical Analysis

Each experiment was carried out three times, each time in triplicate (n = 3). Data are reported as mean $\pm$ SD. The different groups/conditions were compared by one-way or two-way analysis of variance (ANOVA) and Tukey–Kramer post hoc test; a p value < 0.05 was considered to denote a statistically significant difference between experimental and control groups. Statistical analysis and graph design were carried out by means of GraphPad Prism 7.00 software (GraphPad Inc., San Diego, CA, USA).

3. Results

3.1 Verb and C3G Recover the Viability of HREC Grown under HG Conditions

The effects of increasing amounts of C3G and Verb, or their association were evaluated on HREC cell viability cultured for 48 h under NG (5 mM) or HG (25 mM) conditions. Initially, cell viability was tested under NG conditions in order to evaluate the tolerability of the antioxidant compounds at the concentration of 5, 10 and 50 μM tested individually or in association. As shown by the white bars in Fig. 2, none of these doses produced significant changes in HREC viability in comparison with control conditions (vehicle alone). As expected, [18] cell exposure to HG for 48 h decreased by about 25% HREC viability (grey bars). Such an effect is not the mere consequence of the increased osmolarity, because we had already shown that a similar concentration of mannitol had no toxic effects and did not

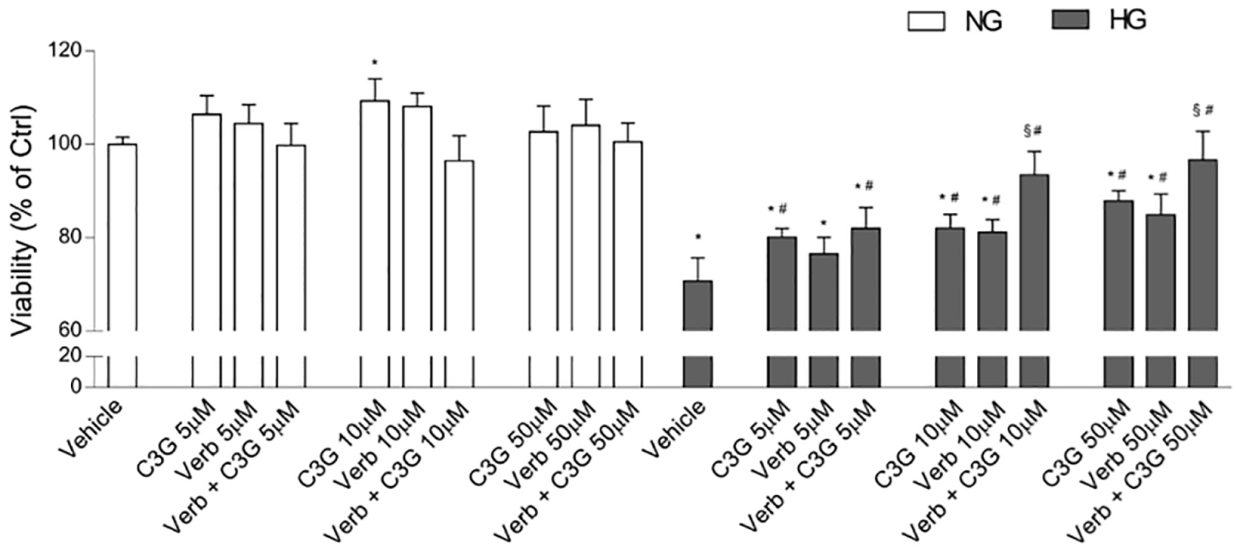

Fig. 2. Effects of C3G and Verbascoside on HG-induced damage on HREC. Cell viability was evaluated by the MTT assay in cells after 48 h of growth in cell culture medium with normal glucose (NG, 5 mM: white bars) or with high glucose (HG, 25 mM: grey bars). NG or HG media also contained increasing amounts (5, 10 and 50 μM) of C3G or Verbascoside (Verb) or an equimolar association of both compounds. Control samples were grown under NG or HG conditions and with no additions (labeled as Vehicle). Data are shown as mean $\pm$ SD of three independent experiments, each one run in triplicate. *$p < 0.05$ vs Vehicle; #$p < 0.05$ vs HG; §$p < 0.05$ vs HG plus single compounds at the same concentration.

change the observed parameters [18]. At each increasing concentration of C3G or Verb (5, 10 and 50 μM) under HG conditions we observed a progressive increase of cell viability. At the highest dose of 50 μM C3G or Verb prevented the reduction of cell viability induced by HG by about 60 and 45%, respectively ($p < 0.05$). Interestingly, while at the lower concentration of 5 μM there was no cooperative effect of the two molecules combined together, at the higher doses of 10 and 50 μM a clear significant advantage of the association over the single molecules was evident, increasing the protective effect by 40% at 10 μM, and around 30% at 50 μM.

3.2 Verb and C3G Blunt ROS Production in HREC Grown with HG

Endothelial damage induced by the presence of HG follows the intracellular accumulation of ROS within HREC. Consistently with the decrease in cell viability, HG more than doubled the amount of intracellular ROS in HREC (Fig. 3 and Table 1). The concomitant presence of C3G or Verb had a dose-dependent effect in decreasing the amount of ROS, respectively by 44% and 25%. The association of the two molecules at 10 and 50 μM gave a further protection, however, plateauing at around 50%.

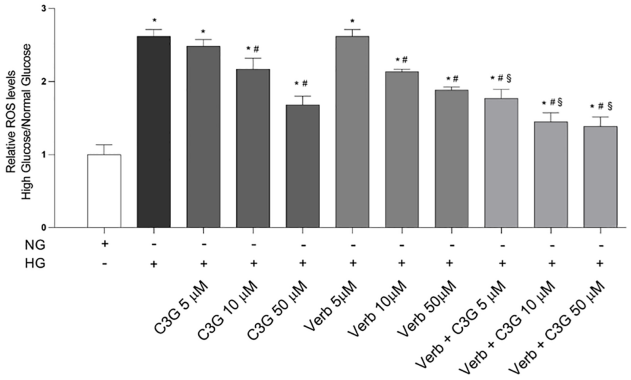

Fig. 3. Effects of C3G and Verbascoside on HG-induced ROS accumulation within HREC. Relative ROS levels were quantitated by the H2DCFDA assay after 48 h of growth with normal glucose (NG, 5 mM) or with high glucose (HG, 25 mM). NG or HG media also contained increasing amounts (5, 10 and 50 μM) of C3G or Verbascoside (Verb) or an equimolar association of both compounds. Control samples were grown under NG conditions and with no additions (Vehicle). Data are shown as mean $\pm$ SD of three independent experiments, each one run in triplicate. *$p <$ 0.05 vs NG Vehicle; #$p < 0.05$ vs HG; §$p < 0.05$ vs HG plus the single compound at the same concentration.

3.3 C3G and Verb Prevent TEER Reduction in HREC Confluent Monolayers Grown with HG

HG conditions may disrupt the endothelial barrier, causing leakage and edema. In order to evaluate the protective effect of C3G and Verb on the barrier integrity of HREC monolayers upon HG-treatment, we measured the Trans Endothelial Electrical Resistance (TEER). This parameter usually provides a good *in vitro* estimation of blood-retinal barrier (BRB) integrity [48]. As shown in Fig. 4, shifting the HREC confluent monolayer (at time 0) to HG conditions

Table 1. Intracellular ROS measured in HREC cells under NG or HG conditions.

Treatment	NG (O.D.)	HG (O.D.)
Vehicle	2.87 ± 0.39	7.31 ± 0.22
C3G 5 μM	2.50 ± 0.17	6.20 ± 0.23
C3G 10 μM	2.47 ± 0.42	5.34 ± 0.37
C3G 50 μM	2.46 ± 0.31	4.13 ± 0.30
Verb 5 μM	2.70 ± 0.14	7.23 ± 0.13
Verb 10 μM	2.99 ± 0.34	6.36 ± 0.10
Verb 50 μM	2.91 ± 0.19	5.48 ± 0.12
C3G + Verb 5 μM	2.69 ± 0.54	4.75 ± 0.41
C3G + Verb 10 μM	3.12 ± 0.35	4.52 ± 0.47
C3G + Verb 50 μM	2.40 ± 0.44	3.43 ± 0.69

Reactive oxygen species (ROS) levels measured through the H2DCFDA assay in HREC treated with normal glucose (NG, 5 mM) or with high glucose (HG, 25 mM) for 48 h. NG or HG media were supplemented with increasing amounts (5, 10 and 50 μM) of C3G or Verbascoside (Verb) or with both compounds and compared to media without compounds (Vehicle). Data are shown as mean ± SD of three independent experiments, each one run in triplicate. O.D., optical density.

causes a progressive decrease of TEER by 40% and 50% of the original value at 48 and 72 h of treatment, as compared to NG conditions, which guarantee a stability of the barrier effect. Treatment with 50 μg/mL of each antioxidant molecule, either alone or in association, was able to significantly prevent such a TEER decrease in HG-treated cells. The lowest protective effect was observed with Verb alone, while C3G alone at 48 and 72 h had a stronger protective effect. The association of the two molecules gave the best protective effect.

3.4 C3G and Verb Prevent the HG-Induced Increase of Paracellular Permeability in a Confluent HREC Monolayer

Increased paracellular permeability of the retinal endothelium represents one of the main hallmarks of the HG-induced cell damage *in vitro*, which mimics the pathological increase in retinal vascular leakage in hyperglycemic conditions [51]. Given the reduction of TEER reported in Fig. 4, likely due to a decrease in tight junctions between endothelial cells, we would expect to also see an increase of paracellular permeability in HREC monolayers after shifting to HG conditions, and a preventive effect of C3G and Verb. We used sodium fluorescein added to the upper well of a transwell plate as a marker to follow leakage from the upper to the lower well. Fig. 5A shows the fluorescein permeation kinetics through an intact endothelial monolayer maintained under NG or shifted to HG conditions, showing a dramatic progressive increase induced by HG throughout the recorded times. The presence of Verb or C3G at 50 μM attenuated this phenomenon, with C3G again more

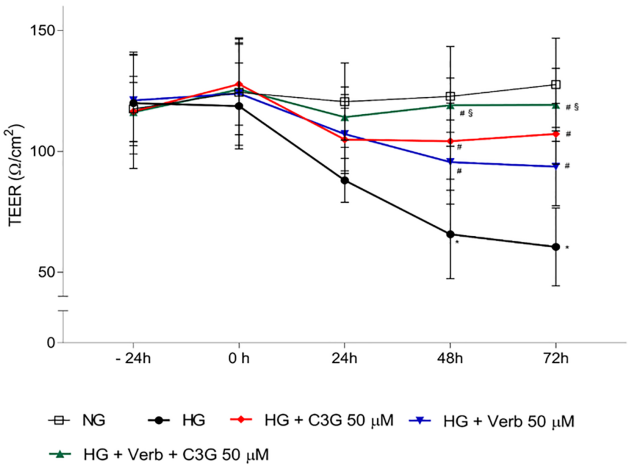

Fig. 4. Effects of C3G and Verbascoside on Trans Endothelial Electrical Resistance (TEER) of HREC monolayers grown under NG or HG conditions with or without C3G and verbascoside. Stable cell monolayers were obtained by culturing the cells in appropriate insert-wells for 5 days. Then, cell monolayers were treated up to 72 h with HG with or without 50 μM C3G, or 50 μM Verbascoside, or 50 μM of both compounds in comparison to NG. TEER values were monitored for the duration of the experiments. Data are shown as a mean ± SD of three independent experiments, each one run in triplicate. *$p < 0.05$ vs NG Vehicle; #$p < 0.05$ vs HG; §$p < 0.05$ vs HG plus the single compound at the same conc.

efficient than Verb, and the association of the two returned leakage to a quasi-normal state. Fig. 5B shows the paracellular permeability index (Pe) extrapolated from data at 5 min, and Fig. 5C shows a good correlation (R = 0.83) obtained between the Pe index (Fig. 4B) and TEER values at 48 h (Fig. 4).

3.5 C3G and Verb Prevent the Down Regulation of Tight Junction Proteins Zonula Occludens-1 (ZO-1) and VE-Cadherin in a Confluent HREC Monolayer Exposed to HG

The effects of HG on the integrity loss of the endothelial barrier had been previously related to changes in the expression and/or the degradation of junction proteins, which may explain the increased leakage under hyperglycemic conditions [52,53]. We show here (Fig. 6A) the immunocytochemical analysis illustrating the abundance and the integrity of the tight junction proteins ZO-1 and VE-cadherin in a confluent HREC monolayer under NG conditions, and their disarrangement and decrease after 48 h with HG. The simultaneous presence under HG conditions of the association of C3G and Verb (50 μM each) completely prevented such effects due to HG. Semiquantitative data of VE-Cadherin and ZO-1 fluorescence intensity are respectively presented in Fig. 6B,C, coherently with what appears in the illustrative pictures and showing almost full restoration by C3G and Verb of the junctional proteins. The diffuse staining with ZO-1 of HREC at a late passage *in vitro*

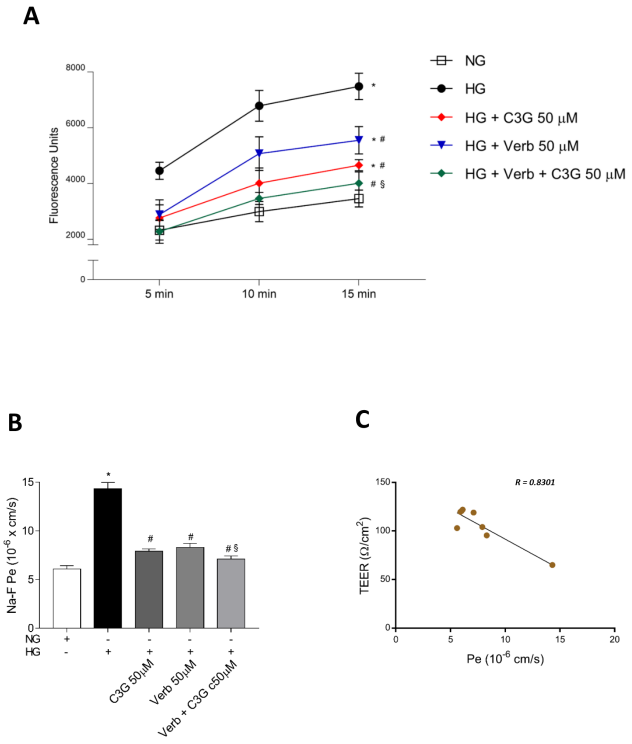

Fig. 5. Effects of C3G and Verbascoside on the HG-induced increase of the paracellular permeability in a confluent monolayer of HREC evaluated by the sodium fluorescein (Na-F) assay. Stable cell monolayers were obtained by culturing the cells in appropriate insert-wells for 5 days. (A) Na-F assays were performed in HREC monolayers treated for 48 h with HG with or without 50 μM of C3G, 50 μM of Verbascoside, or 50 μM of both compounds in comparison to NG. (B) Pe was estimated from the paracellular permeability of the sodium fluorescein (Na-F) assay (Fig. 5A). (C) Correlation between the mean values of TEER and Pe observed under the different experimental conditions examined. The correlation coefficient (R) was calculated with GraphPad Prism 7 for Windows using the function linear fit dose-response interpolation of unknown parameters. The graph was obtained by multiple determinations. Data are shown as a mean ± SD of three independent experiments, each one run in triplicate. *$p < 0.05$ vs NG Vehicle; #$p < 0.05$ vs HG; §$p < 0.05$ vs HG plus the single compound at the same conc.

is not unexpected, and has already been described for brain microvascular endothelial cells [54]. However, even at an advanced passage, HREC could form a tight barrier, showing elevated TEER values and a reduced passage of Na-F (Figs. 4,5). HG still induced a decrease of around 40% of TEER as could be expected from early passage cells [55], and an increased permeability to Na-F, both susceptible to rescue by C3G and verbascoside, thus demonstrating the reliability of this model system. Consistently with the above immune-fluorescent data, a further demonstration of C3G and Verb capability to preserve BRB-like properties of the HREC confluent monolayer is given in Fig. 7, in which we evaluated by western blot analyses (Fig. 7A) the amount of ZO-1 and VE-Cadherin under different growth conditions (NG or HG) with or without the addition of 50 μM of C3G, Verb or their association. These data confirm that ZO-1 and VE-Cadherin protein levels were reduced by about 70 and 50%, respectively ($p < 0.05$) in HG-treated HREC monolayers compared to NG control cells (Fig. 7B,C). The presence of C3G, or Verb, or both compounds together did not alter ZO-1 and VE-Cadherin protein levels under NG conditions. However, C3G or Verb at a concentration of 50 μM prevented the decrease of junction protein expression by HG, and when given together maintained their expression at control levels.

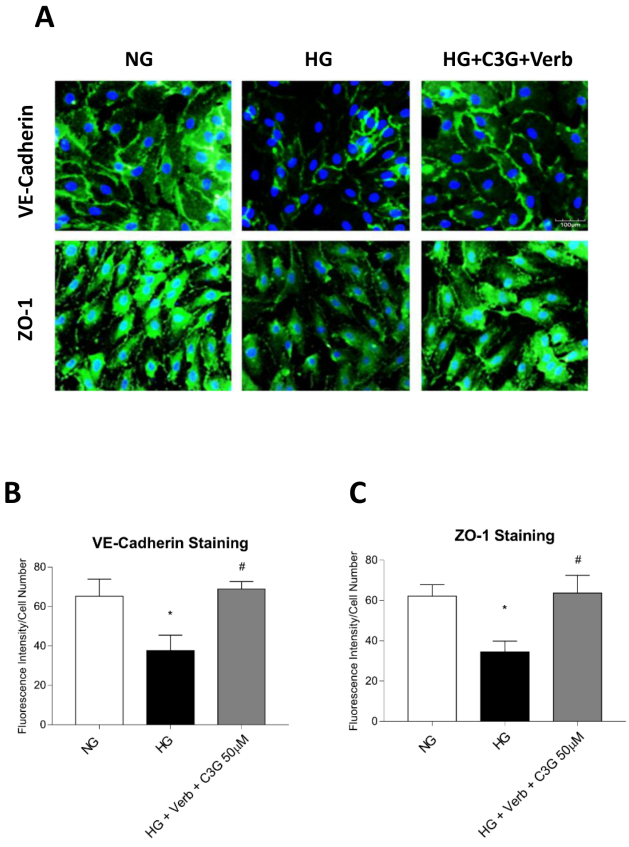

Fig. 6. Effect of C3G and Verbascoside on the HG-induced down-regulation of endothelial tight junction proteins evaluated by immunocytochemical analysis. Confluent monolayers of HREC were treated for 48 h with HG with or without 50 μM C3G plus Verbascoside in comparison to NG. (A) representative images of immunocytochemical staining performed using specific antibody against VE-cadherin and ZO-1 proteins. Intensity of immunoreactivity for VE-cadherin (B) and ZO-1 (C) was measured using Image J program analyzing randomly selected fields for each replicate. Data are shown as a mean ± SD of three independent experiments, each one run in triplicate. *$p < 0.05$ vs NG Vehicle; #$p < 0.05$ vs HG; §$p < 0.05$ vs HG plus the single compound at the same conc.

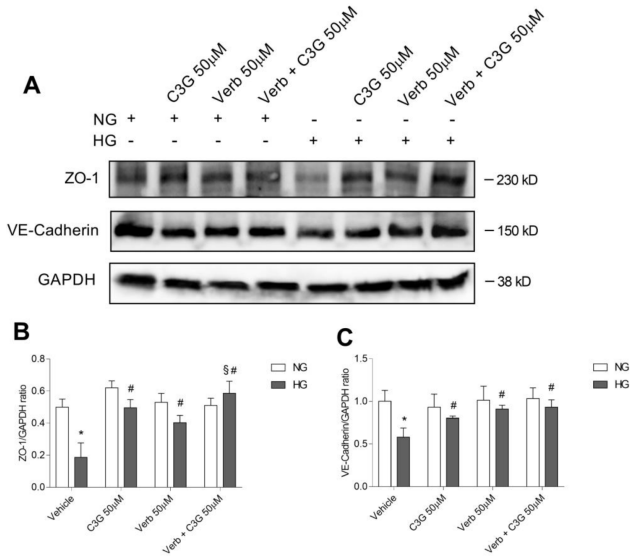

Fig. 7. Effects of C3G and Verbascoside on the HG-induced down-regulation of endothelial tight junction proteins evaluated by western blot analysis. (A) Representative immunoblot performed using specific antibodies against ZO-1 and VE-cadherin on lysates from confluent monolayers of human retinal endothelial cells (HREC) treated for 48 h with HG with or without 50 μM of C3G, 50 μM of Verbascoside, or 50 μM of both compounds compared to NG. (B) and (C) bar graphs representing densitometric measure of ZO-1 and VE-cadherin protein bands normalized against the relative housekeeping GAPDH protein level. Loading was 40 μg per lane. Data are shown as a mean $\pm$ SD of three independent experiments, each one run in triplicate. *$p < 0.05$ vs NG Vehicle; #$p < 0.05$ vs HG; §$p < 0.05$ vs HG plus the single compound at the same conc.

4. Discussion

4.1 The Role of Hyperglycemic Stress

The pathological manifestations of DR are triggered by the overwhelming oxidative stress occurring further to the failure of glycemic control, and mainly involve the microvascular endothelial system. Therefore, the therapeutic approach to prevent or treat DR is based primarily on the control of the glycemic index, because maintaining the glycosylated hemoglobin (HbA1c) level below 7% may decrease the risk of DR development and progression [56]. However, despite the known benefits of improved glycemic control, a large number of diabetic patients do not manage to keep safe blood glucose levels, which together with an adequate surveillance program for the monitoring of hyperglycemia-induced damage, could potentially spare diabetic complications to an elevated number of patients [57].

4.2 The Medical Need

In their advanced stages, PDR and DME are treated by invasive procedures, such as vitrectomy, intravitreal injections of corticosteroids or anti-VEGF and laser photocoagulation. Such treatments are not curative, and at their best they are aimed at preserving the residual visual ability of the patient [57]. Moreover, several patients are not responders to intravitreal therapies [58]. Hence, there is an urgent medical need to develop new and less invasive therapeutic approaches for the prevention or treatment of DR in order to try and reduce the incidence and progression of this disease, starting from its early stages. Such new therapeutic strategies are not necessarily alternative, but may be associated with surgical treatments in order to complement and improve their efficacy. Therefore, since ROS overproduction in mitochondria is caused by diabetic hyperglycemic stress [59], the attenuation of these events may play a pivotal role in the treatment of DR, preventing or delaying its progression towards the more advanced stage of the disease.

4.3 Antioxidants in Food Supplements May Contribute to Prevention and Treatment

Currently, the International Classification of Diabetic Retinopathy and Diabetic Macular Edema considers the use of antioxidants as potentially effective in the treatment of mild forms of NPDR and DME, while no indications are given for their use in the treatment of PDR [60]. Studies from *in vitro* and *in vivo* models suggest that nutraceuticals may relieve the pathophysiological complications of DR such as inflammation and neurodegeneration, by an enhancement of the antioxidant defense systems and the consequent reduction of ROS accumulation [61,62]. The main dietary antioxidants are found in colored foods, and are represented by polyphenols and carotenoids (Fig. 8). Flavonoids belong to a larger group of natural substances with different phenolic structures, which can be found in different kinds of fruits and vegetables, and their derivatives. They are endowed with anti-inflammatory and antioxidant effects, so that they are nowadays considered indispensable components in several nutraceutical, pharmaceutical, medicinal and cosmetic applications [63]. In several different preclinical and clinical studies, the different classes of flavonoids have shown good efficacy in counteracting the deleterious effects of oxidative stress and inflammation on the retina of diabetic subjects [64,65]. For instance, in HREC stimulated by human retinoblastoma cell line conditioned medium or VEGF, the protective role played by quercetin in counteracting the pro-angiogenic stimulus has been demonstrated [66]. Consistently, data reported in this paper show the protective effects on the BRB of two polyphenolic antioxidants, belonging to different families: cyanidin-3-glucoside is an anthocyanin, and verbascoside is a phenylpropanoid glucoside, a family of molecules mainly found in medicinal plants. We used a primary human retinal endothelial cell line (HREC) to test the protective effects of C3G and Verb when the cells were shifted to HG growth conditions. It was previously shown that HG affects both macro and microvascular endothelial

cells, altering their metabolism, finally resulting in the typical vascular dysfunctions of diabetes and DR [67]. In this respect, BRB efficiency depends on the expression by endothelial cells of junction proteins such as VE-Cadherin and ZO-1, which are downregulated in the presence of high glucose conditions [68]. Therefore, strategies have been described to counteract such a decrease and maintain BRB properties. For instance, erythropoietin and tumor necrosis factor ligand-related molecule 1A (TL1A) have been described as factors able to preserve and restore VE-cadherin expression and BRB integrity in the presence of high glucose levels [69,70]. Along this line, Behl [65] and Matos [64] reported that two different polyphenols, scutellarin and curcumin, could contrast the effects on growth and apoptosis of HG conditions, increase the expression of junction proteins and decrease the formation of branched tubular structures. More recently, HREC grown under HG conditions were used to show the effects of fluorometholone (a glucocorticoid drug used in inflammatory and allergic disorders of the eye) in blunting the release of inflammatory cytokines and VEGF, and inhibiting the HG-induced cellular senescence mediated by the Akt pathway [71].

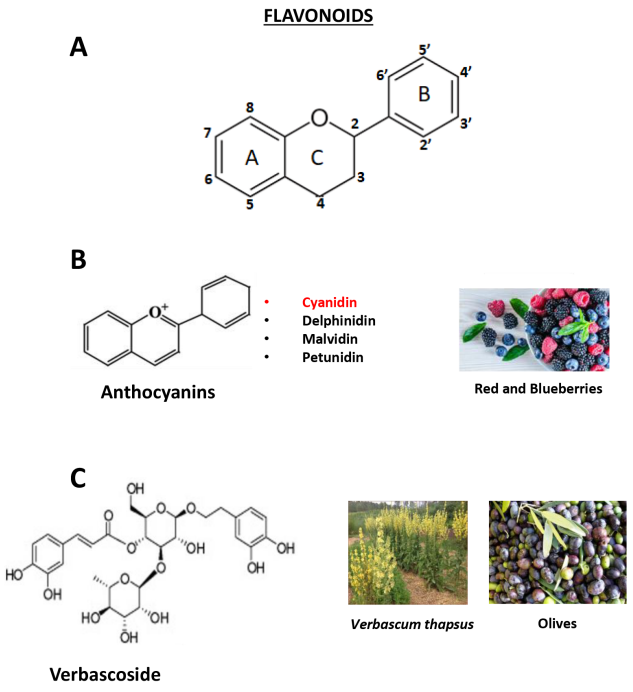

Fig. 8. Molecular structure of the compounds used in this study. The generic structure of flavonoids is illustrated (A), together with the structure of anthocyanins (B), which include the cyanidins such as C3G, and verbascoside (C).

4.4 The Effects of C3G

Under our experimental conditions, HREC monolayers shifted to HG conditions (25 mM) for 48 h showing a dramatic increase of intracellular ROS, concomitant with growth inhibition, a two-fold decrease of TEER correlating with an increased paracellular permeability and a decreased expression of tight junction proteins. All these effects could be efficiently dampened in a dose-dependent way by C3G and Verb or - better - by the combination of the two. Accordingly, C3G has been shown to be able to prevent the disruption of the barrier function of retinal pigmented epithelial cells (RPE) caused by blue light irradiation, besides activating the Nrf2 pathway, thus enhancing endogenous antioxidant protection and promoting RPE survival [72]. In a more comprehensive study addressing DR, C3G suppressed migration, invasion and angiogenesis of HREC and blunted the activation of microglial BV2 cells stimulated *in vitro* by HG [66]; moreover, in diabetic mice induced by streptozotocin the oral treatment with C3G decreased inflammation, microglial activation and angiogenesis in the retina [73]. Moreover, C3G could protect pancreatic beta-cell dysfunction induced by palmitic acid treatment, conserving their secretory function and alleviating apoptosis [74]. Finally, C3G could prevent diabetic cataract formation as suggested by its protective activity on lens epithelial cells *in vitro* exposed to HG conditions [75].

4.5 The Effects of Verbascoside

The phenylethanoid glycoside verbascoside/acteoside is a widespread polyphenolic plant compound, showing several biological properties including strong antioxidant, anti-inflammatory and neuroprotective activities. In fact, it is an efficient ROS scavenger and inhibitor of lipid peroxidation. It also inhibits the inducible NO synthase (iNOS) in the CNS, prevents the activation of COX2 in glioma cells, and protects from inflammatory events by downregulating the activation of the pro-inflammatory transcription factor NFkB, while activating the Nrf2 pathway leading to the endogenous expression of antioxidants, such as HO1 [76]. Similar to what has previously been described for C3G, also Verb can protect pancreatic beta cells from endoplasmic reticulum (ER)-stress mediated dysfunctions, acting on the protein kinase RNA-like endoplasmic reticulum kinase (PERK) branch of the unfolded protein response and enhancing mitochondrial dynamics. As a consequence, beta cells showed increased viability, mitochondrial function and insulin content [77].

4.6 The Association of C3G and Verb

For the first time ever, we have shown in an *in vitro* model system with human microvascular retinal endothelial cells stressed by HG treatment, that the association of C3G and Verb is more efficient than each single molecule in preserving the cells from death and the loss of barrier function, in line with the idea that a pleiotropic action obtained by the combination of different molecules can be more effective than the protection given by the single components [78].

5. Conclusions

In conclusion, we have shown here in an *in vitro* model system with human microvascular retinal endothelial cells that the association of two polyphenols (C3G and verbascoside), belonging to different families, may efficiently prevent the endothelial barrier dysfunction that usually follows diabetic hyperglycemic stress, and is the cause of diabetic retinopathy progression towards the most dangerous proliferative neovascular stage. These data confirm and further support from a biological point of view what had already been shown in an *in vivo* model system of early-stage diabetic retinopathy [45,46].

Availability of Data and Materials

The datasets used and/or analyzed during the current study are available from the corresponding author on reasonable request.

Author Contributions

Conceptualization—DR, GG, CDA, GL; investigation—GG, AL, AC, AA; data curation—GG, CDA and GL; writing - original draft preparation—DR, GG, CDA, GL; writing - review and editing—DR, GG.

Ethics Approval and Consent to Participate

Not applicable.

Acknowledgment

The Authors thank prof. Antony Bridgewood for critical English proofreading of the manuscript.

Funding

This research received no external funding.

Conflict of Interest

DR and GL are serving as Editorial Board members of this journal. We declare that DR and GL had no involvement in the peer review of this article and had no access to information regarding its peer review. Full responsibility for the editorial process for this article was delegated to GP. DR is a full-time employee of Fidia Pharmaceuticals, a pharmaceutical company that commercializes a food supplement containing C3G and verbascoside.

References

[1] Nentwich MM, Ulbig MW. Diabetic retinopathy - ocular complications of diabetes mellitus. World Journal of Diabetes. 2015; 6: 489–499.

[2] Hartnett ME, Baehr W, Le YZ. Diabetic retinopathy, an overview. Vision Research. 2017; 139: 1–6.

[3] Vinores SA. Breakdown of the Blood–Retinal Barrier. Encyclopedia of the Eye. 2010; 216–222.

[4] Romero-Aroca P, Baget-Bernaldiz M, Pareja-Rios A, Lopez-Galvez M, Navarro-Gil R, Verges R. Diabetic Macular Edema Pathophysiology: Vasogenic versus Inflammatory. Journal of Diabetes Research. 2016; 2016: 2156273.

[5] Wilkinson CP, Ferris FL 3rd, Klein RE, Lee PP, Agardh CD, Davis M, *et al*. Global Diabetic Retinopathy Project Group. Proposed international clinical diabetic retinopathy and diabetic macular edema disease severity scales. Ophthalmology. 2003; 110: 1677–1682.

[6] Wang W, Lo ACY. Diabetic Retinopathy: Pathophysiology and Treatments. International Journal of Molecular Sciences. 2018; 19: 1816.

[7] Yamagishi S, Matsui T. Advanced Glycation End Products (AGEs), Oxidative Stress and Diabetic Retinopathy. Current Pharmaceutical Biotechnology. 2011; 12: 362–368.

[8] Ruan Y, Jiang S, Musayeva A, Gericke A. Oxidative Stress and Vascular Dysfunction in the Retina: Therapeutic Strategies. Antioxidants. 2020; 9: 761.

[9] Sies H. Oxidative stress: a concept in redox biology and medicine. Redox Biology. 2015; 4: 180–183.

[10] Münzel T, Camici GG, Maack C, Bonetti NR, Fuster V, Kovacic JC. Impact of Oxidative Stress on the Heart and Vasculature: Part 2 of a 3-Part Series. Journal of the American College of Cardiology. 2017; 70: 212–229.

[11] Lassègue B, Clempus RE. Vascular NAD(P)H oxidases: specific features, expression, and regulation. American Journal of Physiology. Regulatory, Integrative and Comparative Physiology. 2003; 285: R277–R297.

[12] Du Y, Veenstra A, Palczewski K, Kern TS. Photoreceptor cells are major contributors to diabetes-induced oxidative stress and local inflammation in the retina. Proceedings of the National Academy of Sciences. 2013; 110: 16586–16591.

[13] Peng J, Xiong S, Ding L, Peng J, Xia X. Diabetic retinopathy: Focus on NADPH oxidase and its potential as therapeutic target. European Journal of Pharmacology. 2019; 853: 381–387.

[14] Li C, Miao X, Li F, Wang S, Liu Q, Wang Y, *et al*. Oxidative Stress-Related Mechanisms and Antioxidant Therapy in Diabetic Retinopathy. Oxidative Medicine and Cellular Longevity. 2017; 2017: 1–15.

[15] Kang Q, Yang C. Oxidative stress and diabetic retinopathy: Molecular mechanisms, pathogenetic role and therapeutic implications. Redox Biology. 2020; 37: 101799.

[16] Antonetti DA, Klein R, Gardner TW. Diabetic Retinopathy. New England Journal of Medicine. 2012; 366: 1227–1239.

[17] Tang J, Kern TS. Inflammation in diabetic retinopathy. Progress in Retinal and Eye Research. 2011; 30: 343–358.

[18] Giurdanella G, Lupo G, Gennuso F, Conti F, Furno DL, Mannino G, *et al*. Activation of the VEGF-A/ERK/PLA2 Axis Mediates Early Retinal Endothelial Cell Damage Induced by High Glucose: New Insight from an *In vitro* Model of Diabetic Retinopathy. International Journal of Molecular Sciences. 2020; 21: 7528.

[19] Duraisamy AJ, Mishra M, Kowluru A, Kowluru RA. Epigenetics and Regulation of Oxidative Stress in Diabetic Retinopathy. Investigative Opthalmology & Visual Science. 2018; 59: 4831.

[20] Liu J, Chen S, Biswas S, Nagrani N, Chu Y, Chakrabarti S, *et al*. Glucose-induced oxidative stress and accelerated aging in endothelial cells are mediated by the depletion of mitochondrial SIRTs. Physiological Reports. 2020; 8: e14331.

[21] Giurdanella G, Lazzara F, Caporarello N, Lupo G, Anfuso CD, Eandi CM, *et al*. Sulodexide prevents activation of the PLA2/COX-2/VEGF inflammatory pathway in human retinal endothelial cells by blocking the effect of AGE/RAGE. Biochemical Pharmacology. 2017; 142: 145–154.

[22] Anfuso CD, Olivieri M, Fidilio A, Lupo G, Rusciano D, Pezzino S, *et al*. Gabapentin Attenuates Ocular Inflammation: *In vitro* and In vivo Studies. Frontiers in Pharmacology. 2017; 8: 173.

[23] Jo DH, Yun J, Cho CS, Kim JH, Kim JH, Cho C. Interaction between microglia and retinal pigment epithelial cells determines

the integrity of outer blood-retinal barrier in diabetic retinopathy. Glia. 2019; 67: 321–331.
[24] Lv Z, Phuong TA, Jin S, Li X, Xu M. Protection by simvastatin on hyperglycemia-induced endothelial dysfunction through inhibiting NLRP3 inflammasomes. Oncotarget. 2017; 8: 91291–91305.
[25] Navaratna D, McGuire PG, Menicucci G, Das A. Proteolytic degradation of VE-cadherin alters the blood-retinal barrier in diabetes. Diabetes. 2007; 56: 2380–2387.
[26] Semeraro F, Morescalchi F, Cancarini A, Russo A, Rezzola S, Costagliola C. Diabetic retinopathy, a vascular and inflammatory disease: Therapeutic implications. Diabetes & Metabolism. 2019; 45: 517–527.
[27] Rohowetz LJ, Kraus JG, Koulen P. Reactive Oxygen Species-Mediated Damage of Retinal Neurons: Drug Development Targets for Therapies of Chronic Neurodegeneration of the Retina. International Journal of Molecular Sciences. 2018; 19: 3362.
[28] Huang W, Yan Z, Li D, Ma Y, Zhou J, Sui Z. Antioxidant and Anti-Inflammatory Effects of Blueberry Anthocyanins on High Glucose-Induced Human Retinal Capillary Endothelial Cells. Oxidative Medicine and Cellular Longevity. 2018; 2018: 1–10.
[29] Ramirez JE, Zambrano R, Sepúlveda B, Kennelly EJ, Simirgiotis MJ. Anthocyanins and antioxidant capacities of six Chilean berries by HPLC–HR-ESI-ToF-MS. Food Chemistry. 2015; 176: 106–114.
[30] Amorini AM, Lazzarino G, Galvano F, Fazzina G, Tavazzi B, Galvano G. Cyanidin-3-O-beta-glucopyranoside protects myocardium and erythrocytes from oxygen radical-mediated damages. Free Radical Research. 2003; 37: 453–460.
[31] Zhu W, Jia Q, Wang Y, Zhang Y, Xia M. The anthocyanin cyanidin-3-O-β-glucoside, a flavonoid, increases hepatic glutathione synthesis and protects hepatocytes against reactive oxygen species during hyperglycemia: Involvement of a cAMP–PKA-dependent signaling pathway. Free Radical Biology and Medicine. 2012; 52: 314–327.
[32] Serraino I, Dugo L, Dugo P, Mondello L, Mazzon E, Dugo G, *et al*. Protective effects of cyanidin-3-O-glucoside from blackberry extract against peroxynitrite-induced endothelial dysfunction and vascular failure. Life Sciences. 2003; 73: 1097–1114.
[33] Xu JW, Ikeda K, Yamori Y. Cyanidin-3-glucoside regulates phosphorylation of endothelial nitric oxide synthase. FEBS Letters. 2004; 574: 176–180.
[34] Fuji Y, Uchida A, Fukahori K, Chino M, Ohtsuki T, Matsufuji H. Chemical characterization and biological activity in young sesame leaves (Sesamum indicum L.) and changes in iridoid and polyphenol content at different growth stages. PLoS ONE. 2018; 13: e0194449.
[35] Wong IY, He ZD, Huang Y, Chen ZY. Antioxidative activities of phenylethanoid glycosides from Ligustrum purpurascens. Journal of Agricultural and Food Chemistry. 2001; 49: 3113–3119.
[36] Burgos C, Muñoz-Mingarro D, Navarro I, Martín-Cordero C, Acero N. Neuroprotective Potential of Verbascoside Isolated from Acanthus mollis L. Leaves through Its Enzymatic Inhibition and Free Radical Scavenging Ability. Antioxidants. 2020; 9: 1207.
[37] Chiou WF, Lin LC, Chen CF. Acteoside protects endothelial cells against free radical-induced oxidative stress. Journal of Pharmacy and Pharmacology. 2004; 56: 743–748.
[38] Khan RA, Hossain R, Roy P, Jain D, Mohammad Saikat AS, Roy Shuvo AP, *et al*. Anticancer effects of acteoside: Mechanistic insights and therapeutic status. European Journal of Pharmacology. 2022; 916: 174699.
[39] Wang C, Cai X, Wang R, Zhai S, Zhang Y, Hu W, *et al*. Neuroprotective effects of verbascoside against Alzheimer's disease via the relief of endoplasmic reticulum stress in aβ-exposed U251 cells and APP/PS1 mice. Journal of Neuroinflammation. 2020; 17: 309.
[40] Ahmad M, Rizwani GH, Aftab K, Ahmad VU, Gilani AH, Ahmad SP. Acteoside: a new antihypertensive drug. Phytotherapy Research. 1995; 9: 525–527.
[41] Campo G, Marchesini J, Bristot L, Monti M, Gambetti S, Pavasini R, *et al*. The *in vitro* effects of verbascoside on human platelet aggregation. Journal of Thrombosis and Thrombolysis. 2012; 34: 318–325.
[42] Campo G, Pavasini R, Biscaglia S, Ferri A, Andrenacci E, Tebaldi M, *et al*. Platelet aggregation values in patients with cardiovascular risk factors are reduced by verbascoside treatment. a randomized study. Pharmacological Research. 2015; 97: 1–6.
[43] Aldini G, Piccoli A, Beretta G, Morazzoni P, Riva A, Marinello C, *et al*. Antioxidant activity of polyphenols from solid olive residues of c.v. Coratina. Fitoterapia. 2006; 77: 121–128.
[44] Leena MM, Silvia MG, Vinitha K, Moses JA, Anandharamakrishnan C. Synergistic potential of nutraceuticals: mechanisms and prospects for futuristic medicine. Food & Function. 2020; 11: 9317–9337.
[45] Amato R, Canovai A, Melecchi A, Pezzino S, Corsaro R, Dal Monte M, *et al*. Dietary Supplementation of Antioxidant Compounds Prevents Light-Induced Retinal Damage in a Rat Model. Biomedicines. 2021; 9: 1177.
[46] Canovai A, Amato R, Melecchi A, Dal Monte M, Rusciano D, Bagnoli P, *et al*. Preventive Efficacy of an Antioxidant Compound on Blood Retinal Barrier Breakdown and Visual Dysfunction in Streptozotocin-Induced Diabetic Rats. Frontiers in Pharmacology. 2022; 12: 811818.
[47] Zanetta L, Marcus SG, Vasile J, Dobryansky M, Cohen H, Eng K, *et al*. Expression of Von Willebrand factor, an endothelial cell marker, is up-regulated by angiogenesis factors: a potential method for objective assessment of tumor angiogenesis. International Journal of Cancer. 2000; 85: 281–288.
[48] Lupo G, Motta C, Salmeri M, Spina-Purrello V, Alberghina M, Anfuso CD. An *in vitro* retinoblastoma human triple culture model of angiogenesis: a modulatory effect of TGF-β. Cancer Letters. 2014; 354: 181–188.
[49] Kis B, Deli MA, Kobayashi H, Ábrahám CS, Yanagita T, Kaiya H, *et al*. Adrenomedullin regulates blood–brain barrier functions *in vitro*. Neuroreport. 2001; 12: 4139–4142.
[50] Yuan SY, Rigor RR. Regulation of Endothelial Barrier Function. Colloquium Series on Integrated Systems Physiology: from Molecule to Function. 2011; 3: 1–146.
[51] Saker S, Stewart EA, Browning AC, Allen CL, Amoaku WM. The effect of hyperglycaemia on permeability and the expression of junctional complex molecules in human retinal and choroidal endothelial cells. Experimental Eye Research. 2014; 121: 161–167.
[52] Tien T, Barrette KF, Chronopoulos A, Roy S. Effects of High Glucose-Induced Cx43 Downregulation on Occludin and ZO-1 Expression and Tight Junction Barrier Function in Retinal Endothelial Cells. Investigative Opthalmology & Visual Science. 2013; 54: 6518.
[53] Li J, Lu X, Wei L, Ye D, Lin J, Tang X, *et al*. PHD2 attenuates high-glucose-induced blood retinal barrier breakdown in human retinal microvascular endothelial cells by regulating the Hif-1α/VEGF pathway. Inflammation Research. 2022; 71: 69–79.
[54] Fujimoto T, Morofuji Y, Nakagawa S, Kovac A, Horie N, Izumo T, *et al*. Comparison of the rate of dedifferentiation with increasing passages among cell sources for an *in vitro* model of the blood–brain barrier. Journal of Neural Transmission. 2020; 127: 1117–1124.
[55] Gericke A, Suminska-Jasińska K, Bręborowicz A. Sulodexide reduces glucose induced senescence in human retinal endothelial cells. Scientific Reports. 2021; 11: 11532.

[56] Klein R, Klein BE. Relation of glycemic control to diabetic complications and health outcomes. Diabetes Care. 1998; 21: C39–C43.
[57] Calderon GD, Juarez OH, Hernandez GE, Punzo SM, De la Cruz ZD. Oxidative stress and diabetic retinopathy: development and treatment. Eye. 2017; 31: 1122–1130.
[58] Chen YP, Wu AL, Chuang CC, Chen SN. Factors influencing clinical outcomes in patients with diabetic macular edema treated with intravitreal ranibizumab: comparison between responder and non-responder cases. Scientific Reports. 2019; 9: 10952.
[59] Nishikawa T, Edelstein D, Du XL, Yamagishi S, Matsumura T, Kaneda Y, *et al*. Normalizing mitochondrial superoxide production blocks three pathways of hyperglycaemic damage. Nature. 2000; 404: 787–790.
[60] Alfonso-Muñoz EA, Burggraaf-Sánchez de Las Matas R, Mataix Boronat J, Molina Martín JC, Desco C. Role of Oral Antioxidant Supplementation in the Current Management of Diabetic Retinopathy. International Journal of Molecular Sciences. 2021; 22: 4020.
[61] Rossino MG, Casini G. Nutraceuticals for the Treatment of Diabetic Retinopathy. Nutrients. 2019; 11: 771.
[62] Milluzzo A, Barchitta M, Maugeri A, Magnano San Lio R, Favara G, Mazzone MG, *et al*. Do Nutrients and Nutraceuticals Play a Role in Diabetic Retinopathy? A Systematic Review. Nutrients. 2022; 14: 4430.
[63] Panche AN, Diwan AD, Chandra SR. Flavonoids: an overview. Journal of Nutritional Science. 2016; 5: e47.
[64] Matos AL, Bruno DF, Ambrósio AF, Santos PF. The Benefits of Flavonoids in Diabetic Retinopathy. Nutrients. 2020; 12: 3169.
[65] Behl T, Kumar K, Singh S, Sehgal A, Sachdeva M, Bhatia S, *et al*. Unveiling the role of polyphenols in diabetic retinopathy. Journal of Functional Foods. 2021; 85: 104608.
[66] Lupo G, Cambria MT, Olivieri M, Rocco C, Caporarello N, Longo A, *et al*. Anti-angiogenic effect of quercetin and its 8-methyl pentamethyl ether derivative in human microvascular endothelial cells. Journal of Cellular and Molecular Medicine. 2019; 23: 6565–6577.
[67] Duffy A, Liew A, O'Sullivan J, Avalos G, Samali A, O'Brien T. Distinct effects of high-glucose conditions on endothelial cells of macrovascular and microvascular origins. Endothelium. 2006; 13: 9–16.
[68] Fresta CG, Fidilio A, Caruso G, Caraci F, Giblin FJ, Leggio GM, *et al*. A New Human Blood-Retinal Barrier Model Based on Endothelial Cells, Pericytes, and Astrocytes. International Journal of Molecular Sciences. 2020; 21: 1636.
[69] Liu D, Xu H, Zhang C, Xie H, Yang Q, Li W, *et al*. Erythropoietin maintains VE-cadherin expression and barrier function in experimental diabetic retinopathy via inhibiting VEGF/VEGFR2/Src signaling pathway. Life Sciences. 2020; 259: 118273.
[70] Li J, Xie R, Jiang F, Li Y, Zhu Y, Liu Z, *et al*. Tumor necrosis factor ligand-related molecule 1a maintains blood–retinal barrier via modulating SHP-1-Src-VE-cadherin signaling in diabetic retinopathy. The FASEB Journal. 2021; 35: e22008.
[71] Zhou X, Wang L, Zhang Z, Liu J, Qu Q, Zu Y, *et al*. Fluorometholone inhibits high glucose-induced cellular senescence in human retinal endothelial cells. Human & Experimental Toxicology. 2022; 41: 9603271221076107.
[72] Peng W, Wu Y, Peng Z, Qi W, Liu T, Yang B, *et al*. Cyanidin-3-glucoside improves the barrier function of retinal pigment epithelium cells by attenuating endoplasmic reticulum stress-induced apoptosis. Food Research International. 2022; 157: 111313.
[73] Zhao F, Gao X, Ge X, Cui J, Liu X. Cyanidin-3-o-glucoside (C3G) inhibits vascular leakage regulated by microglial activation in early diabetic retinopathy and neovascularization in advanced diabetic retinopathy. Bioengineered. 2021; 12: 9266–9278.
[74] Chen Y, Li X, Su L, Hu Q, Li W, He J, *et al*. Cyanidin-3-O-Glucoside Ameliorates Palmitic-Acid-Induced Pancreatic Beta Cell Dysfunction by Modulating CHOP-Mediated Endoplasmic Reticulum Stress Pathways. Nutrients. 2022; 14: 1835.
[75] Song XL, Li MJ, Liu Q, Hu ZX, Xu ZY, Li JH, *et al*. Cyanidin-3-O-glucoside Protects Lens Epithelial Cells against High Glucose-Induced Apoptosis and Prevents Cataract Formation via Suppressing NF-κB Activation and Cox-2 Expression. Journal of Agricultural and Food Chemistry. 2020; 68: 8286–8294.
[76] Tatli I, Kahraman C, Akdemir Z. The Therapeutic Activities of Selected Scrophulariaceae and Buddlejaceae Species and Their Secondary Metabolites Against Neurodegenerative Diseases. Bioactive Nutraceuticals and Dietary Supplements in Neurological and Brain Disease: Prevention and Therapy. 2015; 95–111.
[77] Galli A, Marciani P, Marku A, Ghislanzoni S, Bertuzzi F, Rossi R, *et al*. Verbascoside Protects Pancreatic β-Cells against ER-Stress. Biomedicines. 2020; 8: 582.
[78] Rusciano D, Pezzino S, Mutolo MG, Giannotti R, Librando A, Pescosolido N. Neuroprotection in Glaucoma: Old and New Promising Treatments. Advances in Pharmacological Sciences. 2017; 2017: 4320408.